

THE EFFECT OF HEAT TREATMENT ON THE OPTICAL PROPERTIES OF COPPER-CONTAINING LITHIUM-POTASSIUM-BORATE GLASSES

P.S. Shirshnev¹, V.L. Ugolkov², Zh.G. Snezhnaia¹, D.I. Panov¹,
E.V. Shirshneva-Vaschenko¹, S.N. Lipnitskaya¹, A.E. Romanov¹
and V.E. Bougrov¹

¹ITMO University, Kronverkskiy prospect 49, Saint-Petersburg, 197101, Russia

²Grebenshchikov Institute of Silicate Chemistry, Russian Academy of Sciences, Tiflisskaya str 3, Saint-Petersburg, 199034, Russia

Received: May 12, 2018

Abstract. The paper presents the investigation of lithium-potassium-alumoborate glasses (0-25 mol.% Li₂O) doped by copper ions. The effect of glass annealing on the Raman scattering patterns is discussed. It is shown that such an annealing results in drastic changes in the Raman scattering patterns for the glass with 10 mol.% of Li₂O: the band at 481 cm⁻¹ conventionally attributed to boron-oxygen bonds in metaborate rings disappears, while a set of narrow bands at 1236, 1500, and 1783 cm⁻¹ is observed. We consider one of these bands, 1783 cm⁻¹, as being the identifier of the formed Li(Al₇B₄O₁₇) nanophase, XRD analysis supported the above suggestion. The effect of newly formed nanophase on the luminescence spectra is discussed.

1. INTRODUCTION

One of the interesting features of borate glasses is the possibility of nanophase formation as a result of glass annealing at temperatures above the glass transition temperature. It should be noted that nanophase formation here couples with the ability of the boron ion to exist in two different structural environment (trigonal and tetrahedral [1]) affecting the glass luminescence spectra. Such an effect was previously shown for potassium – alumina – borate glasses with manganese ferrite [2], iron ferrite [3], and copper chloride [4-6] nanophases formed as a result of glass annealing.

The effect of copper ions doping could be described as follows: UV excitation in range from 320 up to 400 nm results in monovalent copper ions and their clusters broadband luminescence in optical media that occupies almost all the visible range [7].

The use of this property is important for fiber and volumetric spark sensors [8], ultraviolet dosimeters [9], white LEDs [10], and down converters for solar cells [11]. As shown in [12,13], potassium-alumina-borate glasses doped by with copper ions and clusters possess the thermochromic luminescence, the glass heating up to 200 °C results in the luminescence wavelength shift of 100 nm.

Generally, the quantum yield of luminescence related to copper ions in borate glasses can reach 50% [14]. The luminescence excitation in lithium-potassium-alumina-borate glasses with monovalent copper ions in the glass matrix was reported in [15]. In [16], authors discussed the glass annealing effect on the luminescence of chromium-containing lithium-potassium-alumina-borate glasses; the formation of the luminescent Li(Al₇B₄O₁₇) phase with the typical peaks at 685, 700, and 715 nm was

Corresponding author: P.S. Shirshnev, e-mail: pavel.shirshnev@gmail.com

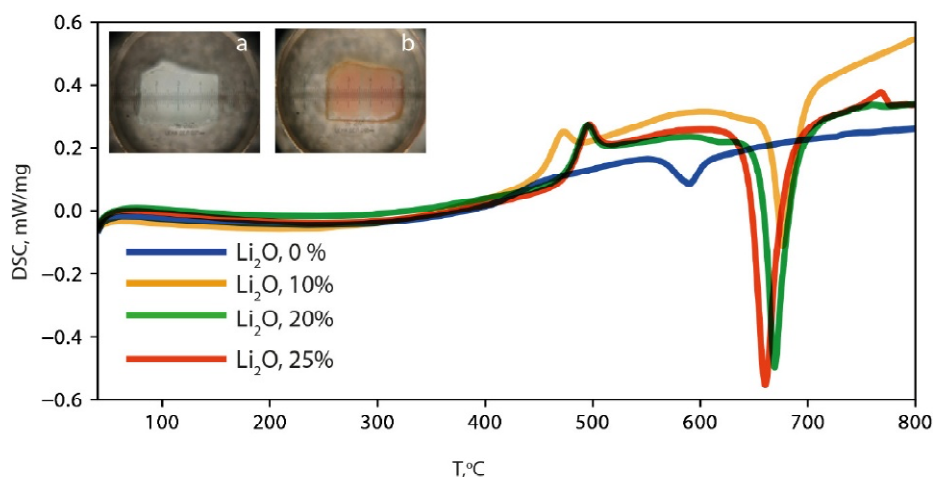


Fig. 1. DSC curves of studied samples. Insets: a – photo of the sample without Li_2O before the annealing, b – after the annealing.

stated; the quantum yield here was estimated as being more than 50%. The authors considers that in $\text{Li}(\text{Al}_7\text{B}_4\text{O}_{17})$ phase here can be doped with chromium.

Since the effect of copper ion doping can be considered as similar to that observed in the case of chromium addition, the task of the present work was to study the effect of glass annealing on the luminescent characteristics of copper-doped lithium-borate glasses. Coupling scanning calorimetry, XRD analysis, and Raman spectroscopy, we have investigated the changes in the glass structure and proved the nanophase formation as the result of glass annealing. We believe that such studies will provide additional information on glass structure transformations at annealing above the glass transition temperature.

2. EXPERIMENTAL

Glasses with $(25-x)\text{K}_2\text{O}-x\text{Li}_2\text{O}-25\text{Al}_2\text{O}_3-50\text{B}_2\text{O}_3$ ($x=0, 10, 20,$ and 25 mol.%) composition were synthesized; copper doping was performed as follows: extra 0.5 wt.% of Cu_2O was added to the each glass batch composition before the synthesis. Lithium-free $(25\text{K}_2\text{O}-25\text{Al}_2\text{O}_3-50\text{B}_2\text{O}_3)$ glass without copper additions was used as a reference sample. All glasses were baked at 1400°C in air for 2 hours, then the glass melt was poured out onto a metal plate. At the final step, the glasses were cooled in a muffle furnace from 400°C to room temperature for 12 hours in air.

Synthesized glasses were studied by differential thermal analysis (DSC, STA 429 CD NETZSCH), as a result, glass transition temperatures and temperature ranges of crystallizations were determined.

The measurements were conducted in the temperature range from 50 to 800°C in air atmosphere with heating rate of $10^\circ\text{C}/\text{min}$.

Phase identification and structure determination were carried out using X-ray diffraction (XRD) techniques (DRON-8 X-ray diffractometer, $\text{Cu}_{\text{K}\alpha 1}$ radiation, 40 kV, 20 mA, $\lambda=0.154$ nm).

For further measurements, flat-parallel samples of synthesized glasses were prepared. The Raman spectra were excited by the radiation of a polarized 50 Wt power helium-neon laser ($\lambda=633$ nm); the spectra were recorded using a single pass Renishaw spectrometer. The photoluminescence emission spectra were measured with Avantes Avaspec 2048 spectrometer at 320 nm excitation wavelength.

3. RESULTS AND DISCUSSION

Fig. 1 shows the results of DSC studies. As seen from the figure, the glass transition temperature of the glass without Li_2O is 400°C , the further temperature increase demonstrates the exothermic peak at 589°C . Note that the reference sample with the same chemical composition but without copper oxide addition (not shown in Fig. 1) thermogram did not contain any exothermic peaks, though the glass transition temperature remained the same. The values of glass transition and crystallization temperatures for samples studied are given in Table 1.

From the visual inspection and comparison of the glasses studied, one can see that the glass without lithium has been crystallized after DSC measurements; its color transferred into a dark red (Fig. 1b). As reported in [15], such a color is typical for the glass containing copper nanoparticles. Thus,

Table 1. Glass transition and crystallization temperatures of studied glasses.

Li ₂ O, mol.%	Glass transition temperature, °C	Temperature of crystallization, °C
0	400	589
10	422	676
20	446	669
25	449	660

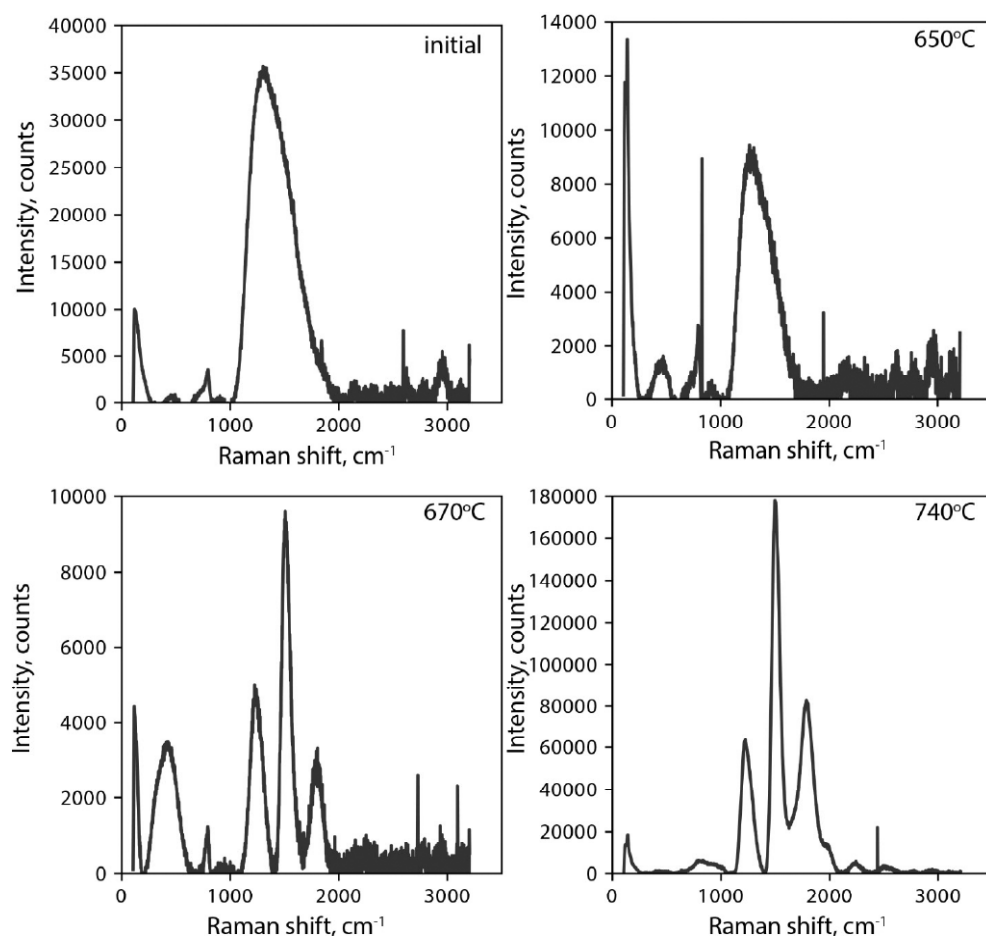
one can suppose that metal copper nanoparticles are formed at 589 °C, this effect manifests itself as an exothermic effect at the DSC curve.

Analyzing the data registered for the other glasses, one can conclude that the addition of lithium oxide caused drastic transformation of DSC curves. In particular, the addition of 10 mol.% Li₂O shifted the glass transition temperature to higher values (up to 450 °C). In addition, the exothermic peak attributed above to the crystallization was also found to be shifted to upper temperatures (676 °C). However, the further increase in the lithium oxide contents

leads to the lower temperatures of the exothermic effect, at that, the intensity of the peak increases. It can be assumed that that this increase in the peak intensity is directly proportional to the concentration of lithium oxide. The maximum thermal effect for glass crystallization was achieved at 660 °C for the glass in which potassium was completely replaced with lithium (i.e., glass with 25 mol.% Li₂O). Hence, as follows from DSC data, lithium promotes crystalline phase formation, this conclusion agrees the reference data [13]. Thus, one can expect that the glass annealing at proper temperatures will cause the similar crystalline phase formation.

We have chosen the glass with 10 mol.% of Li₂O for the further studies. To investigate the annealing effect on the samples luminescent properties, the samples were isothermally annealed at 650, 670, and 740 °C for 20 min.

Fig. 2 depicts Raman scattering spectra of samples before (“initial glass”) and after annealing. Let us discuss these data in some more detail. The Raman spectra registered for the initial glass and for the sample annealed at 650 °C are quite similar.

**Fig. 2.** Raman spectra of samples with 10 mol.% Li₂O contents before the annealing (“initial glass”) and after the annealing at 650, 570, and 740 °C.

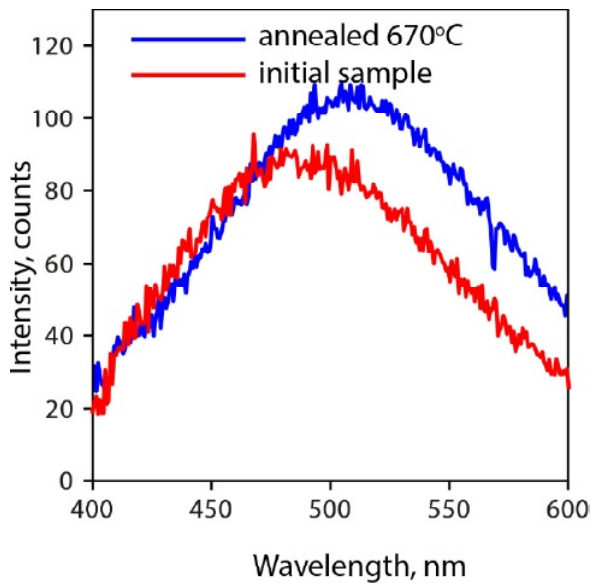


Fig. 3. Photoluminescence spectra of sample with 10 mol.% Li_2O contents before and after the annealing.

However, the annealing temperature increase up to 670 °C resulted in the drastic changes of the Raman scattering curve changes, these changes are also observed for the sample annealed at higher (740 °C) temperature. As seen from Fig. 2, wide bands at 1481 cm^{-1} , 793 cm^{-1} , and 461 cm^{-1} are observed in the initial glass and for the sample annealed at 650 °C Raman spectra. For the samples annealed at higher temperatures (670 and 740 °C) the wide band at 1481 cm^{-1} was changed to 1236 cm^{-1} , 1500, and 1783 cm^{-1} bands. Note that the temperature of 670 °C corresponds to the crystallization peak at the DSC curve (Fig. 1), one can conclude this temperature as a critical one for the Raman spectrum transformation.

Regarding for the above conclusion, the sample annealed at 670 °C was chosen for the further studies. The data on sample photoluminescence at the excitation wavelength of 320 nm were obtained and compared with the same data for the initial glass, see Fig. 3. As seen from this figure, the annealing procedure shifts the wavelength of the photoluminescence peak from 493 nm to 510 nm.

Fig. 4 demonstrates the results of XRD analysis of the sample annealed at 670 °C. As seen from the figure, some amount of amorphous phase is present in the sample studied along with the crystalline phase, it's analysis gives an opportunity to identify it as $\text{Li}(\text{Al}_7\text{B}_4\text{O}_{17})$. Calculations done using Sherrer's equation [17] give an opportunity to estimate the average size of crystalline particles as ~20 nm, hence, the formed $\text{Li}(\text{Al}_7\text{B}_4\text{O}_{17})$ phase can be considered as a nanophase.

Following Ref. [18], the Raman spectrum band at 1481 cm^{-1} is identified as being associated with longitudinal vibrations of boron-oxygen bonds in metaborate rings and chains and, also, as the band of piroborate groups. The band at 793 cm^{-1} corresponds to the deformation vibrations of boron – oxygen – boron. The band at 461 cm^{-1} is the indicator of the isolated diborate group presence. According to the analysis provided in Ref. [18], bands at 1236 cm^{-1} and 1500 cm^{-1} correspond to trigonal boron groups and to longitudinal B-O metaborate rings, respectively. However, current literature does not contain data about 1783 cm^{-1} Raman scattering band registered in boron- or copper-containing crystals or glasses. We propose that this band corresponds to $\text{Li}(\text{Al}_7\text{B}_4\text{O}_{17})$ phase (see XRD data in Fig. 4 and discussion above) and can be used for its identification.

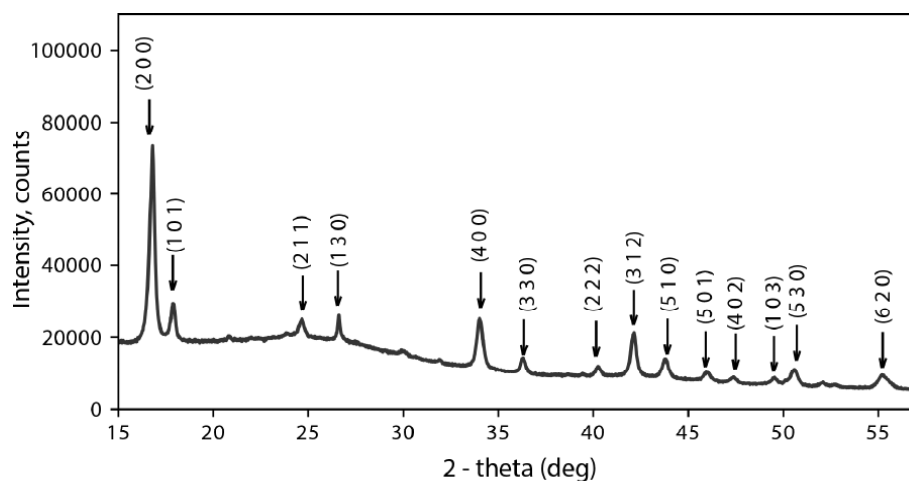


Fig. 4. X-ray diffraction patterns of sample with 10 mol.% Li_2O contents after the annealing at 670 °C. Main peaks of $\text{Li}(\text{Al}_7\text{B}_4\text{O}_{17})$ nanophase are marked by arrows.

Comparing our results with the data reported in [16], we can also assume that three different bond types (bonds in trigonal boron groups, longitudinal B-O bonds in metaborate rings, and bonds causing 1783 cm^{-1} Raman band) form three different types of environment for chromium ions studied in [16]. In turn, this results in three different photoluminescence bands at 685 nm, 700 nm, and 715 nm in the glass.

According to Ref. [15], the wide photoluminescence bands in Fig. 3 correspond to the band of monovalent Cu^+ copper ions. The red shift of photoluminescence peak wavelength is then explained by the fact of nanocrystal formation in glass with associated changes in the environment of copper ions. This leads to the photoluminescence spectra transformation and to the luminescence maximum shift by 25 nm.

4. CONCLUSION

We have observed the formation of $\text{Li}(\text{Al}_7\text{B}_4\text{O}_{17})$ nanophase at potassium-lithium-borate copper-containing glass after annealing at 670 °C. Precipitating of the nanophase in the glass modifies the environment of copper ions affecting the luminescence spectra and causing the changes in the Raman scattering spectra. Raman spectrum of annealed glass has one new non-identified before line at 1783 cm^{-1} , we assume that this line corresponds to $\text{Li}(\text{Al}_7\text{B}_4\text{O}_{17})$ phase.

ACKNOWLEDGEMENTS

Research was conducted under the support of the Russian Science Foundation, Grant no. 17-72-10216.

REFERENCES

- [1] J. Zhong and P.J. Bray // *Journal of Non-Crystalline Solids* **111** (1989) 67.
- [2] I. Edelman, O. Ivanova, I. Ivantsov, D. Velikanov, E. Petrakovskaja, A. Artemenko, J. Curély, J. Kliava, V. Zaikovskiy and S. Stepanov // *IOP Conference Series: Materials Science and Engineering* **25** (2011) 012017.
- [3] O.S. Ivanova, I.S. Edelman, R.D. Ivantsov, V.N. Zabluda, S.A. Stepanov, S.M. Zharkov, G.M. Zeer, Y.V. Zubavichus, A.A. Veligzhanin and J. Curely // *Bulletin of the Russian Academy of Sciences: Physics* **75** (2011) 707.
- [4] P.S. Shirshnev, N.V. Nikonorov, D.I. Sobolev, A.A. Kim, I.M. Kislyakov, S.S. Povarov and I.M. Belousova // *Journal of Optical Technology* **84** (2017) 705.
- [5] P. Shirshnev, V. Tsekhomskiy and N. Nikonorov, *RU2466107C2 Russian patent* (2012).
- [6] A.N. Babkina, P.S. Shirshnev, N.V. Nikonorov and A.M. Efimov // *Journal of Non-Crystalline Solids* **471** (2017) 362.
- [7] B. Moine, C. Pedrini, E. Duloisy, P. Boutinaud, C. Parent and G. Le Flem // *Journal de Physique IV Colloque* **01** (1991) C7-289.
- [8] D.S. Agafonova, E.V. Kolobkova, A.I. Ignatiev, N.V. Nikonorov, T.A. Shakhverdov, P.S. Shirshnev, A.I. Sidorov and V.N. Vasiliev // *Optical Engineering* **54** (2015) 117107.
- [9] H. El Hamzaoui, Y. Ouerdane, L. Bigot, G. Bouwmans, B. Capoen, A. Boukenter,; S. Girard and M. Bouzaoui // *Optics Express* **20** (2012) 29751.
- [10] N. Uekawa, M. Ouchi, C.M. Wen, T. Matsumoto and T. Kojma // *Journal of the Ceramic Society of Japan* **123** (2015) 924.
- [11] E. Cattaruzza, M. Mardegan, T. Pregolato, G. Ungaretti, G. Aquilanti, A. Quaranta, G. Battaglin and E. Trave // *Solar Energy Materials and Solar Cells* **130** (2014) 272.
- [12] A.N. Babkina, T.S. Kiprushkina, P.S. Shirshnev and N.V. Nikonorov // *Journal of Optical Technology* **83** (2016) 434.
- [13] A.N. Babkina, M.A. Khodasevich and P.S. Shirshnev // *Optics and Spectroscopy* **122** (2017) 214.
- [14] P.S. Shirshnev, A.E. Romanov, V.E. Bougrov, E.V. Shirshneva-Vaschenko and Z.G. Snezhnaia, In: *SPIE Proceedings, Nonference 'Photonics for Solar Energy Systems VII'* (International Society for Optics and Photonics, 2018), 106881D.
- [15] P.S. Shirshnev, Zh.G. Snezhnaia, E.V. Shirshneva-Vaschenko, A.E. Romanov and V.E. Bougrov // *MPM* **40** (2018) 78.
- [16] A.N. Babkina, A.D. Gorbachev, K.S. Zyryanova, N.V. Nikonorov, R.K. Nuryev and S.A. Stepanov // *Optics and Spectroscopy* **123** (2017) 369.
- [17] B. Ingham and M.F. Toney, In: *Metallic Films for Electronic, Optical and Magnetic Applications*, ed. by K. Barmak and K. Coffey (Woodhead Publishing, 2014), p. 3.
- [18] A.K. Yadav and P. Singh // *RSC Advances* **5** (2015) 67583.